International Conference on Mathematics, Computational Methods & Reactor Physics (M&C 2009)
Saratoga Springs, New York, May 3-7, 2009, on CD-ROM, American Nuclear Society, LaGrange Park, IL (2009)

Analysis of SPECT Imaging Simulation Using the TITAN Transport Code

Katherine Keller, Ce Yi, and Alireza Haghighat
Department of Nuclear and Radiological Engineering
University of Florida
202 Nuclear Science Building, PO Box 118300, Gainesville, FL 32611
kkeller@ufl.edu; yice@ufl.edu; haghighat@ufl.edu

ABSTRACT

Simulation of the NCAT heart phantom has recently been done using the hybrid deterministic code TITAN. Single photon emission computed tomography (SPECT) simulation is traditionally done using Monte Carlo codes such as SIMIND. This paper analyzes and compares the results of the SIMIND and TITAN codes for an NCAT heart phantom. Since the SIMIND code does not provide statistical information, runs with varying numbers of particles were used to ensure that the solution had converged for the first energy group (source particle energy bin). SIMIND results for the lower energy groups were determined to be less accurate due to the lack of cross section data and larger statistical uncertainties. The output of the TITAN code was analyzed for the Diamond Differencing with zero fix-up (DDZ) and Directional Theta-Weighted (DTW) differencing schemes and various orders of quadrature. The DTW method was found to converge to a solution at a lower order of quadrature than DDZ. In comparison with SIMIND, the DDZ and DTW methods were found to be equally accurate. The SIMIND and TITAN solutions were in good agreement and TITAN was shown to have a much shorter run time than SIMIND.

Key Words: SPECT, imaging, TITAN

1. INTRODUCTION

Single photon emission computed tomography (SPECT) imaging uses an internalized radionuclide as a source. A target organ uptakes a pharmaceutical that has been tagged with a radionuclide. Gamma cameras then capture projection images at various angles around the patient. With data acquired at a sufficient number of angles, the projections can be reconstructed to form a 3-dimensional image of the source. SPECT is considered a functional imaging modality because the source distribution in the body provides information about how it is functioning. In this paper, the uptake of Tc-99m in the myocardium is simulated in a phantom generated by the NURBS-based cardiac-torso (NCAT) [1] code, in which the organs are based on non-uniform rational B-splines (NURBS).

To simulate a SPECT image, Monte Carlo codes such as SIMIND [2] are generally used. However, the hybrid deterministic code TITAN [3] has recently been used to simulate SPECT imaging of the NCAT heart phantom. These simulations can provide opportunities to improve real SPECT images.

This paper examines the TITAN code's results in the simulation of a SPECT image of the NCAT heart phantom with the variation of the quadrature order and differencing scheme. Further analysis was performed on the SIMIND results for comparison with TITAN.

2. DESCRIPTION OF MODELS

SPECT is frequently used to examine myocardial perfusion by injecting a radiopharmaceutical into the blood supply. The uptake of the radiopharmaceutical into the walls of the heart allows for evaluation of coronary artery disease and heart muscle damage from myocardial infarction. This imaging technique was modeled using an NCAT generated phantom in both the SIMIND and TITAN codes. The parameters used in NCAT, SIMIND, and TITAN are discussed in this section.

The Tc-99m source decays by isomeric transition to emit a 140.5 keV gamma ray. The energy range (10 keV - 154.55 keV) was partitioned into three energy bins with lower bounds of 126.45, 98.35, and 10 keV. A 3-group cross section library was generated by the CEPXS code [4] for use by TITAN. The first energy group bin (126.45-154.55 keV) was chosen based on the detector energy window for a Tc-99m source.

2.1. The NCAT Phantom

The NCAT code was used to generate the phantoms input into the SIMIND and TITAN codes. NCAT is able to create torso phantoms with heart motion. We used the phantom of the first frame (end-diastole) of the heart motion cycle. Default organ sizes were used with total phantom dimensions of 40x40x40 cm^3. A pixel size of 0.62x0.62x0.62 cm^3 was used in the 64x64x64 voxel phantom. The 128x128x128 voxel phantom used a pixel size of 0.31x0.31x0.31 cm^3. There were thirteen materials in the model: air, body (water), intestine, lung, rib bone, liver, kidney, spine bone, muscle, cartilage, spleen, heart, and blood. The NCAT code outputs two phantom volumes: an attenuation distribution containing the material densities and a source distribution containing source strengths in the appropriate voxels.

2.2. The SIMIND Code

As previously discussed, Monte Carlo codes are traditionally used in SPECT simulation. The SIMIND code is specifically designed to simulate SPECT and allows the user to specify details about the model. To obtain results for different energy groups, the SIMIND code allows for windowing, however this means that the simulation must be run from scratch for each energy group. For input, the SIMIND code needs a parameter file detailing the problem, a material density phantom and a source phantom. It is worth noting at this point that the only information about the phantom materials provided to SIMIND is their densities. The output contains the simulated projection images at each angle. To better match with TITAN's parameters, the SIMIND code's built-in collimator simulation was turned off, allowing selection of a photon solid angle (0.0115 radians) within the code.

While SIMIND is an established code that will be used to determine the accuracy of the TITAN code's results, it does not provide any statistical information in its output. To verify that the code had indeed converged to a solution, runs with increasing numbers of particles were compared. This enabled estimation of the number of particles needed for an accurate solution.

2.3. The TITAN Code

TITAN is a 3-D hybrid deterministic transport code and was applied to SPECT simulation for this paper. The TITAN code allows users to apply either a discrete ordinates (S_N) solver or a method of characteristics (MOC) solver in different regions of a model. Applied to SPECT, the TITAN code uses the S_N method in the phantom and a ray-tracing formulation in the collimator region. This ray tracing algorithm was developed for low scattering media. The TITAN code does not currently model a collimator. Collimator blur was incorporated by integrating the angular flux over the same collimator solid angle used in SIMIND [3].

Input for the TITAN code includes the NCAT attenuation and source phantoms as well as the appropriate material cross-sections. TITAN can perform calculations for all energy groups in one run. The TITAN output includes flux moment distributions as well as the projection images at the requested angles. TITAN has the advantage of finding a solution in the form of flux moments, which can then be use to generate as many projection images as desired without solving the problem all over again.

3. RESULTS AND ANALYSIS

In order to compare various projection images, each projection was normalized to its highest pixel value. In the images, it is clear that peripheral pixels will receive few counts, if any. These low count pixels are in unimportant regions far from the source and will have large errors. For this reason, numerical comparisons between projections were confined to normalized pixels with values greater than 0.65 in the heart region. This cutoff value was chosen to restrict our analysis to the high count pixels in the myocardium.

Projection images were compared quantitatively using the infinity-norm and 2-norm given by equations (1) and (2), respectively.

$$\text{Infinity} - \text{norm} = \max[(P'_{ij} - P_{ij})/P_{ij}] \tag{1}$$

$$2 - \text{norm} = \left[\sum_{i,j}\left(\frac{P'_{ij} - P_{ij}}{P_{ij}}\right)^2\right]^{1/2} \tag{2}$$

3.1. SIMIND Results

The SIMIND simulation was run for each of the three specified energy groups using the 64x64x64 pixel phantom. When displayed, groups 2 and 3 revealed inaccuracies in the SIMIND solution. These lower energy groups are comprised of scattered radiation. Denser and higher Z materials, like bone, will greatly reduce the number of photons reaching the detector compared with soft tissue due to photoelectric absorption. The anterior projection images produced by SIMIND for 1 million particles per projection and TITAN for S6-DTW are displayed in Figure 1 for each energy group. Figure 1(c) shows the SIMIND result for group 3, however the expected attenuation in bone is not seen and the photons appear to have simply spread out in the phantom. Figure 2(c) shows the TITAN group 3 results with the sternum and ribs clearly visible. The

SIMIND input does not include any cross sections and so its calculations are based on its knowledge of the material densities. This limited information appears to leave SIMIND unable to accurately represent energy groups lower than the one containing the source. For this reason, further analysis on the SIMIND data will be performed for the first energy group only.

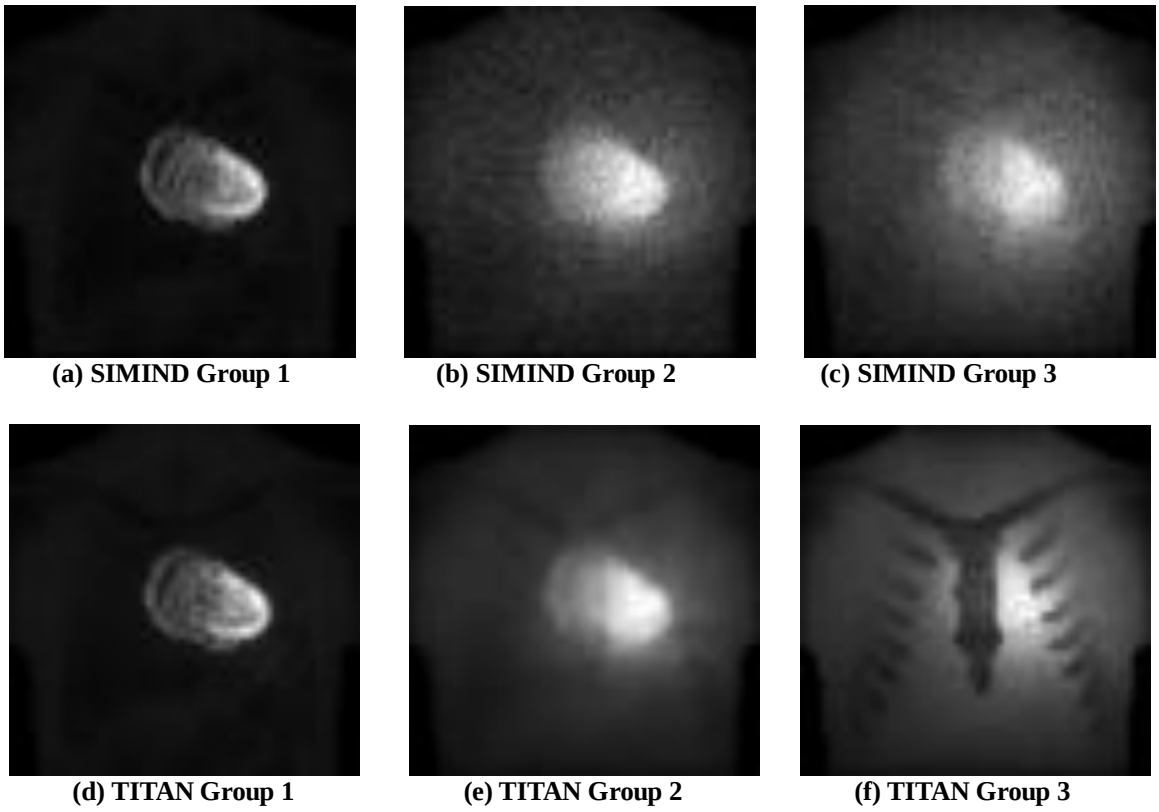

(a) SIMIND Group 1 **(b) SIMIND Group 2** **(c) SIMIND Group 3**

(d) TITAN Group 1 **(e) TITAN Group 2** **(f) TITAN Group 3**

Figure 1. Three group anterior projection images.

The accuracy of the SIMIND code's solution was evaluated by increasing the number of photons per projection image and comparing results. A run of 131 million photons per projection was assumed to give the correct solution and the error of projection images with fewer photons was calculated relative to it. Here, we consider cases with different numbers of photons including 0.263, 0.526, 0.789, 1.05, 2.63, 5.26, 7.89, 10.5, 52.6, and 131 million photons per projection. For each comparison the infinity-norm was used to demonstrate the maximum difference along with the 2-norm to better represent the entire image difference. These results are plotted as a function of photons per projection in Figure 2.

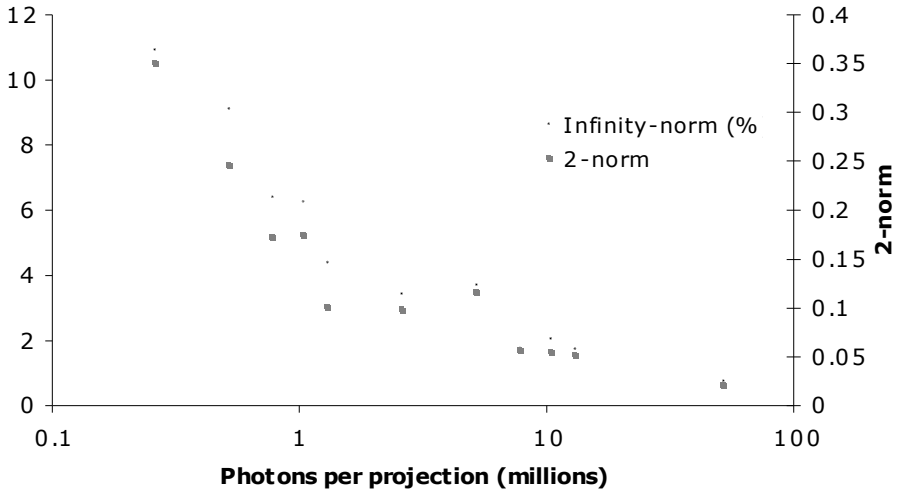

Figure 2. Error relative to 131 million photons per projection.

The trend in Figure 2 shows that the SIMIND solution is converging. It is also clear that the 2-norm values follow the same trend as the infinity-norm. The appropriate number of photons per projection needed will depend on the level of accuracy desired, but we determine about 1 million to be appropriate.

3.2. TITAN Results

The sensitivity of the TITAN code's results to quadrature order and differencing scheme was investigated with the 64x64x64 and 128x128x128 NCAT heart phantoms. The Diamond Differencing with zero fix-up (DDZ) [5] and Directional Theta-Weighted (DTW) [6] schemes were used in conjunction with quadrature orders of S_4, S_6, S_8, S_{10}, and S_{12}. After normalizing each projection image, the number of counts in each pixel in the myocardium was compared. The convergence criterion for the TITAN calculations was set to 1.0×10^{-3}.

The effect of varying the order of quadrature was investigated in group 1 for each differencing scheme and pixel size. Table I displays the results for each quadrature order relative to the next order above it.

Table I. Comparison* between myocardium pixels in group 1 anterior projection images with increasing order of quadrature for different number of pixels (meshes).

Differencing Scheme	Quadrature	64 by 64 by 64		128 by 128 by 128	
		Infinity-norm	2-norm	Infinity-norm	2-norm
DDZ	S_4	1.27%	0.0280	1.12%	0.0718
	S_6	0.56%	0.0119	0.55%	0.0281
	S_8	0.24%	0.0071	0.25%	0.0167
	S_{10}	0.18%	0.0050	0.18%	0.0147
	S_{12}	-	-	-	-
DTW	S_4	0.85%	0.0207	0.95%	0.0532
	S_6	0.43%	0.0099	0.43%	0.0197
	S_8	0.19%	0.0059	0.18%	0.0119
	S_{10}	0.10%	0.0029	0.11%	0.0071
	S_{12}	-	-	-	-

*The norms are calculated by comparing each quadrature order to the next order above it.

The above table demonstrates that for either number of pixels, the DTW differencing scheme converges to its solution at a lower order of quadrature than the DDZ method. Both differencing schemes maintained similar infinity-norms between the 64x64x64 and 128x128x128 phantoms. This finding indicates that for this problem, i.e., considered mesh sizes, both methods are adequate. Based upon the relative error between quadrature orders, S_6 was determined to be appropriate for comparison with SIMIND.

3.3. TITAN Comparison to SIMIND

The results from the TITAN code for S_6-DTW and S_6-DDZ were compared with the most accurate SIMIND result (131 million particles per projection). Figure 3 displays the normalized projection images of the heart produced by each code side-by-side for comparison. Visually, the images are in good agreement.

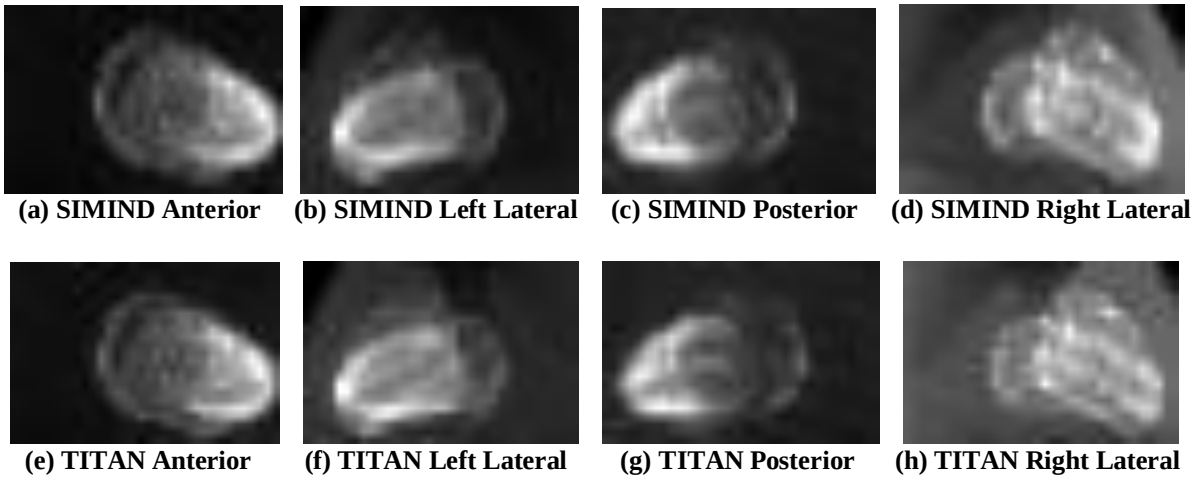

Figure 3. SIMIND and TITAN projection images of heart.

The infinity-norm and 2-norm for TITAN S_6-DDZ and S_6-DTW relative to SIMIND with 131 million particles per projection for four projection angles are presented in Table II.

Table II. Relative error of TITAN S_6-DDZ and S_6-DTW compared to SIMIND for 131 million particles per projection.

Projection Angle		Anterior	Left Lateral	Posterior	Right Lateral
DDZ	Infinity-norm	15.4%	38.3%	32.4%	41.9%
	2-norm	0.445	0.605	0.906	1.19
DTW	Infinity-norm	20.1%	39.5%	28.6%	41.0%
	2-norm	0.575	0.649	0.875	1.13

Numerically, the image infinity-norms and 2-norms for S_6-DDZ and S_6-DTW were similar and ranged from 15.4% for the anterior with DDZ to 41.9% for the right lateral with DDZ. The heart is closest to the anterior surface of the body and so this projection is expected to be more accurate than other angles. Comparing the DDZ and DTW results reveals that neither method is better than the other for this model. A likely contributor to the difference between the TITAN and SIMIND images is the fact that SIMIND uses attenuation values provided in the NCAT phantom, while cross sections were generated separately for TITAN. Further, the large difference in the right lateral image could be attributed to a higher expected uncertainty for the SIMIND calculations. The run times for each code to create four projection images are compared in Table III for a few sets of parameters.

Table III. Three group run time comparison for 4 projection angles.

Code	Time (minutes)	Speedup Factor
SIMIND (131 million particles)	499.6	1
SIMIND (1 million particles)	15.7	31.8
TITAN (S_6-DDZ)	8.6	58.1
TITAN (S_6-DTW)	9.1	54.9

As the above table shows, the TITAN code was able to complete the runs in significantly less time than SIMIND, however the time is highly dependent on the number of photons per projection simulated in SIMIND. The TITAN code's speedup over SIMIND will further improve if the number of projection angles simulated is increased. The DDZ scheme was 30s faster than the DTW method, which could become a reason to use DDZ for larger problems since their accuracy appears to be equal for this case. However, this is for comparing the methods using the same mesh size and, in principle, the DTW scheme could be more efficient than DDZ when run with larger mesh sizes. Future work will investigate this.

3. CONCLUSIONS

The SIMIND Monte Carlo code does not have scattering cross sections as an input and so lower energy groups not containing a source are not accurately represented. The DTW differencing scheme in TITAN shows smaller differences between increasing orders of quadrature than the DDZ method. Both methods were found to be adequate for the 64x64x64 and 128x128x128 mesh sizes. Comparisons between SIMIND and TITAN for DDZ and DTW did not reveal a preferred differencing scheme. DTW is expected to perform better than DDZ for smaller numbers of meshes (i.e., larger mesh sizes) and further studies are needed to see if this is true. The differences between SIMIND and TITAN could be the result of different inputs. For a 64x64x64 phantom and three energy groups, the TITAN code can find a four projection solution over fifty times faster than SIMIND with 131 million particles per projection. With further investigation, the information gained in SPECT simulation could be used to improve real SPECT images. This improvement could result in a better diagnosis and a reduced activity needed to obtain the image.

ACKNOWLEDGMENTS

The authors would like to thank Dr. M. Ljungberg from Lung University, Sweden, for his aid in the use of the SIMIND code.

REFERENCES

1. W. P. Segars, "Development and application of the new dynamic NURBS-based cardiac-torso (NCAT) phantom," PhD Thesis, University of North Carolina (2001).
2. M. Ljungberg, "The SIMIND Monte Carlo program: A Monte Carlo Calculation in Nuclear Medicine," *Applications in Diagnostic Imaging*, **11**, pp.145-163 (1998).

3. C. Yi and A. Haghighat, "SPECT Imaging Simulation Using the TITAN Transport Code," *Proc. M&C 2009*, Saratoga Springs, NY (2009).
4. L. J. Lorence, J. E. Morel, and G. D. Valdez, "User's Guide to CEPXS/ONELD: A One-Dimensional Coupled Electron-Photon Discrete Ordinates Code Package," Sandia National Laboratory (1989).
5. B. Petrovic and A. Haghighat, "Analysis of Inherent Oscillations in Multidimensional S_N Solutions of the Neutron Transport Equation," *Nuclear Science and Engineering*, **124**, pp.31-62 (1996).
6. B. Petrovic and A. Haghighat, "New Directional Theta-Weighted Sn Differencing Scheme," *Transactions of the American Nuclear Society*, **73**, pp.195-197 (1995).